Published in final edited form as:
Langmuir. 2011 January 18; 27(2): 529–537. doi:10.1021/la1020324.

Versatile Small Molecule Motifs for Self-assembly in Water and Formation of Biofunctional Supramolecular Hydrogels

Ye Zhang, **Yi Kuang**, **Yuan Gao**, and **Bing Xu***
Department of Chemistry, Brandeis University, Waltham, MA 02453, USA

Abstract

This article introduces new structural motifs (referred as "samogen") that serve as the building blocks of hydrogelators for molecular self-assembly in water to result in a series of supramolecular hydrogels. Using a compound that consists of two phenylalanine residues and a naphthyl group (also abbreviated as NapFF (**1**) in this text) as an example of the samogens, we demonstrated the ability of the samogens to convert bioactive molecules into molecular hydrogelators that self-assemble in water to result in nanofibers. By briefly summarizing the properties and applications (e.g., wound healing, drug delivery, controlling cell fate, typing bacteria, and catalysis) of these molecular hydrogelators derived from the samogens, we intend to illustrate the basic requirements and promises of the small molecule hydrogelators for applications in chemistry, materials science, and biomedicine.

Keywords

Self-assembly; hydrogels; enzymes; supramolecular; biofunctions; nanofibers; taxol; bisphosphonate; glucosamine; samogen

1. Introduction

Self-assembly is ubiquitous in nature, ranging from the generation of sand dunes to the formation of double helices of deoxynucleotide acid (DNA).1 The exploration of self-assembly at molecular level has offered scientists a powerful strategy (i.e., "bottom-up" method) to develop a range of materials for many useful applications.2،3 One kind of these materials is supramolecular hydrogels as the consequence of self-assembly of certain small molecules (referred to as "supramolecular hydrogelators" or "molecular hydrogelators)4،5،6 in water to form matrices or networks of nanofibers that immobilize water. Although self-assembly and hydrogelation are two separate phenomena, the formation of a supramolecular hydrogel is resulted from the self-assembly of the hydrogelators in water. Unlike polymeric hydrogels7 resulted from the network of cross-linked random polymer chains, supramolecular hydrogels have three subtle but advantageous features. (i) Despite the random entanglement of the nanofibers, the molecular arrangement displays a significant order within the nanofibers (as a form of secondary structure). (ii) The relatively easy structural modification of the small molecules allows tailoring of the molecular order within the nanofibers. And more importantly, (iii) small molecules are more accessible to enzymes and more easily to be converted into hydrogelators according to biochemical cues.6 Molecular hydrogels bear some similar features to those of extracellular matrix (ECM) and

CORRESPONDING AUTHOR Tel: 781-736-5201, Fax: 781-736-2516. bxu@brandeis.edu.

Supporting Information Available: The CIF file of the crystal structure of **1** and additional schemes and figures are available free of charge via the Internet at http://pub.acs.org.

respond to a wide range of stimuli, thus supramolecular hydrogels are attractive for generating new biomaterials for tissue engineering, drug delivery, and other applications.5,8

Although molecular hydrogelators share common features, such as amphiphilicity and supramolecular interactions (for example, π-π interactions, hydrogen bonding, and charge interactions among the molecules) that contribute to the formation of nanostructures and the three-dimensional networks as the matrices of hydrogels, it remains a challenge to predict whether a molecule can act as a hydrogelator. This challenge, unfortunately, limits the research capability for exploring new molecular hydrogelators for desirable applications. One short-term solution to this currently intractable problem is to start the molecular design with a motif known to self-assemble for generating ordered nanostructures in water and promoting hydrogelation. We refer such kind of motifs as "samogens" within the context. A samogen represents the fundamental unit of a molecule that promotes self-assembly. Among the samogens used for making hydrogels, a few oligomeric peptides (with and without lipid-like structures) have received the most extensive exploration and (probably) are the most successful ones up-to-date, especially in the development of biomaterials.9 Despite some successes achieved, the oligomeric peptide-based molecular hydrogelators are expensive and still have to be prepared via multiple step synthesis, which limits the exploration of these molecules as samogens for constructing a wide range of supramolecular materials.

In this article, we introduce a simple samogen, compound **1** (abbreviated as NapFF in this text), which can be easily prepared in the gram scale. Particularly, we demonstrate the ability of **1** to convert bioactive molecules into molecular hydrogelators (Scheme 1) and summarize the properties and applications of these NapFF-derived molecular hydrogelators. We arrange the content of this article in the following way. First, we analyze the structural uniqueness of **1** to elucidate the molecular anatomy, properties of hydrogelation, and possible self-assembled superstructure of this samogen. Second, we briefly illustrate the capability of **1** for enabling other biofunctional molecules to self-assemble in water as the molecular hydrogelators that exhibit useful properties for applications. Third, we offer several anecdotal examples of molecular hydrogelators (Scheme 3) derived from the samogens that share the features displayed by **1**. In last section, we summarize the versatility of the samogens discussed and the general challenges associated with the exploration of molecular hydrogelators.

2. NapFF as a building block for effective molecular self-assembly in water

Like the discovery of other molecular gelators,10 the investigation of NapFF (**1**) also originated from a serendipitous finding that a simple dipeptide protected by fluorenylmethyloxycarbonyl (FMOC), FMOC-Ala-Ala, self-assembles in water to form nanofibers and result in a supramolecular hydrogel.11 This result suggests that aromatic-aromatic interaction not only acts as a stabilizing force for the structures of proteins,12 but also offers a powerful strategy for promoting the self-assembly of small molecules in water to form hydrogels.13 To take the advantage of the aromatic-aromatic interaction in water, we chose to make a dipeptide derivative (i.e., NapFF) that consists of significant amount of aromatic rings. We connected 2-(naphthalen-2-yl) acetic acid with Phe–Phe because (i) the X-ray diffraction data of a β-amyloid analogue14 and the solid state NMR of a seven-residue peptide of Aβ15 indicated that the amyloid core likely contains the hydrophobic Phe-Phe residues for aggregation and (ii) Phe-Phe self-assembles to form nanotubes.16

As shown in Scheme S1, the synthesis of NapFF (**1**) is quite simple and straightforward. L-phenylalanine reacts with N-hydroxysuccimimide (NHS) activated ester of 2-(naphthalene-2-yloxy) acetic acid to afford (S)-2-(2-(naphthalene-2-yl)acetamido)-3-phenylpropanoic acid (NapF). Then, NHS assisted coupling between NapF and L-

phenylalanine gives the pure compound of (S)-2-((S)-2-(2-(naphthalen-2-yl)acetamido)-3-phenylpropanamido)-3-phenylpropanoic acid (NapFF, **1**) in 70% yield after flash column chromatography.

Compound **1** itself also behaves as a molecular hydrogelator and exhibits the critical gelation concentration (cgc) as low as 0.4 wt% (0.83 mM) according to the inverting test tube method, which agrees with the observation that the Phe-Phe motif is prone to self-assembly in water.16 As shown in Figure 1A, **1** forms a transparent hydrogel in water, which undergoes reversible gel-sol transition at about 323 K. A transmission electron micrograph (TEM) reveals that **1** self-assembles to generate nanofibers with widths of 18–45 nm and lengths longer than a few microns (Figure 1B). Further negative staining TEM (Figure 1C) suggests that the fibrils, with the width of 8.5±2.5 nm, twists together to form the nanofibers.

To understand the molecular arrangement of **1** within the nanofibers, we grew the crystal of **1** from its ethanol solution. Although it is unknown whether the obtained crystal structure exactly reflects molecular packing in the nanofibers of the hydrogel, the intermolecular interactions revealed in the single crystal should offer a valuable insight on the possible molecular superstructures of the nanofibers because the local environment of the nanofibers should be quite hydrophobic, which may bear resemblance of the nucleation of **1** in a non-aqueous polar solvent (e.g., ethanol in this case). As shown in Figure 2, all the hydrogen bonding donors and acceptors participate in the formation of intermolecular hydrogen bonds (H…X = 1.74~2.00 Å). The C=O at the N-terminal of **1** form a hydrogen bond with the C-terminal NH of another molecule of **1** (Figure 2A). Although the molecules appear to have “antiparallel” order (being viewed from a-axis), each molecule of **1** aligns crosses two other molecules of **1** and forms hydrogen bonds with them. Being viewed from b-axis (Figure 2B), these crosses extend along the a-axis. As shown in Figure 2C, the COOH of **1** form two hydrogen bonds with the NH and C=O in the middle of another molecule of **1**. At the same time, its own middle section NH and C=O form a pair of hydrogen bonds with the COOH from a different molecule of **1**. Overall, each molecule of **1** can form six hydrogen bonds with four neighboring molecules of **1** (Figure 2D). The capability to form multiple hydrogen bonds with multiple partners possibly facilitate the self-assembly of **1**.

Besides displaying the possible modes of the hydrogen bonding originated from the amide bonds and the carboxylic acid group of **1**, the crystal structure of **1** reveals extensive aromatic-aromatic interactions between the aromatic rings along both a-axis and b-axis (with the average ring distance of 5.31 Å). As shown in Figure 2D, the naphthyl group of **1** interacts with the middle phenyl group of its neighboring molecules of **1** at the same plane. The middle phenyl group simultaneously interacts with the terminal phenyl group of the molecules of **1** below and above. Reciprocally, the terminal phenyl group of the molecule of **1** interacts with the middle phenyl group of a pair of the molecules of **1** below and above. Thus, each molecule of **1** interacts with six neighboring molecules of **1** via the aromatic-aromatic interaction. These aromatic-aromatic interactions not only facilitate long range order of the molecules, but also provide the hydrophobic environment that may cooperatively reinforce the intermolecular hydrogen bonding between the molecules of **1** even in water, thus greatly increasing the self-assembly tendency of **1** to form nanofibers and hydrogels. Overall, it is likely that the extensive multiple interactions, including hydrogen bonds and aromatic-aromatic interactions, among the molecules of **1** enhance their self-assembly in water, which makes **1** an exceptionally efficient “samogen”.

3. Molecular hydrogelators based on NapFF

The capability of **1** to form multiple non-covalent interactions with several partners suggests that **1** should be able to promote molecular self-assembly in water after it conjugates with bioactive or other molecules, though such conjugation could cost a few non-covalent interactions due to the loss of carboxylic acid at the C-terminal and/or the increase of the steric congestion at the side of **1**. Figure 3 shows two modes for conjugating **1** to a bioactive molecule: “end-on” or “side-on”. In this section, we start the discussion with the “end-on” mode because they were explored prior to the “side-on” mode (although the “side-on” samogen might be more versatile).

NapFF-aminobisphosphonate (2)

To evaluate the functions and applications of bisphosphonate based hydrogels, we conjugated **1** to a bisphosphonate in “end-on” mode. Bisphosphonates are small molecules with a P–C–P structure that has structural similarities to the P–O–P structure of pyrophosphate. The P–C–P and P–O–P groups both show high affinity with calcium phosphate crystal surfaces and their binding to these surfaces inhibits further calcium phosphate accretion or dissolution. Thus, bisphosphonates are potent inhibitors of bone resorbing cells (osteoclasts) and are of clinical benefit in a variety of metabolic bone disorders.17 Besides the applications for bone diseases, phosphate group on the bisphosphonate exhibits high affinity to uranyl cations. Therefore, hydrogels, consisting of bisphosphonate group for binding to uranium and other transuranium metal ions, may provide unique advantages for the treatment of wounds contaminated with radionuclides because (i) nanofibers have high surface/volume ratio to provide excellent binding capacity; and (ii) hydrogels should confine the radioactive uranium to the wound in contrast to liquid-based treatments because they barely flow. These potential applications of bisphosphonate based hydrogels lead us to conjugate **1** to a bisphosphonate in “end-on” mode. Scheme S2 shows the synthetic procedure, a HBTU assisted coupling reaction links tetraethyl 3-amino-propane-1,1-bisphosphonate with **1** in DMF to afford the ester-protected compound in 55% yield. The subsequent deprotection by the treatment of TMSBr yield **2** in a good yield (51%).

As expected, compound **2** self-assembles in water to result in a molecular hydrogel at the concentration of 1.0 wt%. Typically, the hydrogel (Figure 4A) forms upon carefully adjusting the pH of the solution from 10 to 6.5. The hydrogels are stable at room temperature for months. According to the TEM images of the hydrogel of **2**, the hydrogel contains irregular fibers with widths ranging from 30 nm to about 250 nm, and the fibers show strong tendency to aggregate into bundles and leave large pores in the matrices of the gel.

We administered the hydrogel of **2** on wound sites at the backs of mice after contamination of the wounds by uranyl nitrate, and found that the survival rates of mice improved significantly and the body weight recovered to normal after treatment with the hydrogel.18 Although the applications of the hydrogel of **2** still remain to be fully established, the further development of this type of hydrogels could provide a general strategy for removing toxic substances (e.g., radionuclides or chemical poisons) from external wound sites on human bodies. Moreover, the supramolecular hydrogels should allow the incorporation of other therapeutics to produce multifunctional hydrogels for the topical treatment of various wounds.

NapFF-tyrosine phosphate (3a) and NapFF-tyrosine (3b)

The connection of **1** to tyrosine not only provides an example of the hydrogelator via "end-on" modification, but also greatly expands the scope of the applications of the hydrogelators because it allows enzymatic formation of the hydrogelators and molecular hydrogels. As shown in Figure S1A, it is quite simple and easy to make the precursor (**3a**) of the hydrogelator (**3b**). After the activation of NapFF by NHS, the coupling between NapFF-NHS with O-phospho-tyrosine at a weak basic condition affords the precursor (**3a**). According to the rheological measurement, the addition of acid phosphatase (5.88 U/ml) to the aqueous solution of **3a** (0.5 wt%) triggers immediate hydrogelation to afford a transparent hydrogel. Two hours after adding the enzyme, 84.4% of **3a** transform into **3b**. The TEM image (Figure S1C) shows quite uniform nanofibers (20~40 nm) in the enzymatically-formed hydrogels.

Besides being converted into **3b** by the acid phosphatase, **3a** also serves as the substrate of alkaline phosphatase. As shown in Figure 5, an alkaline phosphatase converts **3a** to **3b**, which leads to the formation of nanofibers and results in hydrogelation. The addition of alkaline phosphatase to a phosphate saline buffer (PBS) solution of **3a** (0.5 wt%, 6.91 mM) affords a hydrogel. Rheological tests reveal that the hydrogel starts to form almost instantly after adding the phosphatase at room temperature, as indicated by the storage modulus (G') dominating the loss modulus (G") (Figure 5A). According to HPLC analysis, about 48% of **3a** transformed to **3b** at the gelling point. The transparency of hydrogel **3b** (Figure 5B) suggests that no microcrystalline aggregates formed in the hydrogel to scatter visible light. The TEM image of the hydrogel (Figure 5C) shows that the diameter of the nanofibers formed by the self-assembly of **3b** is around 26 nm. The addition of the phosphatase to solutions containing different concentrations of **3a** (Figure 5D) allows the estimation of the mgc of **3a** between 0.025 and 0.05 wt% (0.35 and 0.69 mM) in the PBS buffer.

Because the molecular weight of **1** is rather low (480 g/mol), which brings down the molecular weight of the molecular precursor (**3a**, m.w. = 723 g/mol). The low molecular weight of **3a** permits passive diffusion and facilitates the exploration of the hydrogelation of small molecules inside a cell (Figure 6).19 The enzyme then converts the precursor into the hydrogelator that self-assembles to form nanofibers, which could induce hydrogelation inside the cells. The hydrogelation may change the viscosity of the cytoplasm and cause stresses to the cell. Using the *E. coli* that overexpress soluble phosphatase as the model system, we treated the *E. coli* with **3a**. When the bacteria overexpress the enzyme (IPTG+), the formation of the nanofibers of **3b** in the bacteria result in the high intracellular concentration of **3b** (Figure 6B), and the subsequent intracellular hydrogelation inhibited the growth of the *E. Coli*.19 Besides as the first example of the intrabacteria formation of a molecular hydrogel, this result suggests that the up-regulated expression or high activity of an enzyme may confer the specificity needed for controlling the cell fate. In addition, these results clearly indicate that compatibility of the samogen (**1**) to enzymatic reaction, that is, **1** exhibits little inhibitory effect towards the enzyme and it can enable the molecular self-assembly in a complicated environment, such as cytosol.

After the hydrogelation, the enzyme remains in the hydrogel and should be functional if there is no inhibition caused by the hydrogelators derived from **1**. Our recent study20 on the catalytic activity of the hydrogel-immobilized acid phosphatase, indeed, has validated this notion. As shown in Figure 7, we chose an acid phosphatase (AP) to catalyze molecular hydrogelation and examined the catalytic activity of the hydrogel-immobilized AP in both organic and aqueous media. Upon the addition of AP to the solution of the precursor (**3a**) at room temperature, the AP catalyzed the hydrolysis of **3a** to produce **3b**, and the self-assembly of **3b** afforded the hydrogel that immobilized the AP. The test of the stability and activity of AP in different solvents reveals that the self-immobilized AP exhibited activity in

chloroform about 100 times greater than the activity of the corresponding free AP in water (Figure 7C). Moreover, the stability of the immobilized AP increases significantly (Figure 7D). This study further demonstrated the versatility of **1**.

NapFF to conjugate with the substrate of kinase/phosphatase

The compatibility of **1** with the phosphatase allows us to explore the use of a kinase/phosphatase switch to regulate supramolecular hydrogels.21 As shown in Scheme 2, we synthesized a pentapeptidic hydrogelator, NapFFGEY (**4b**), which formed hydrogels at 0.6 wt % via the self-assembly of **4b** (Figure 8A). The addition of a tyrosine kinase to the hydrogel in the presence of adenosine triphosphates (ATP) phosphorylates **4b** to give the corresponding peptide tyrosine phosphate (**4a**), thus disrupting the self-assembly to induce a gel-sol phase transition (Figure 8B); treating the resulting solution with a phosphatase dephosphorylates **4a** to form **4b**, thus restoring the self-assembly to form the hydrogel (Figure 8C). TEM image (Figure 8D) also confirmed the formation of the network of the nanotubes. After using an MTT assay to verify the biocompatibility of **4a** or **4b**,21 we injected **4a** in the mice (subcutaneously) and found the formation of supramolecular hydrogel *in vivo* (Figure 8E). As the first demonstration of an enzyme-switch-regulated supramolecular hydrogel and the first formation of supramolecular hydrogels *in vivo* by an enzymatic reaction, this enzyme-catalyzed reversible self-assembly and gelation of the hydrogelators could lead to a new type of medium for drug delivery because it allows the hydrogels to respond to the expressions of specific enzymes associated with certain tissues, organs, or diseases.

NapFF-based hydrogelators for β-lactamase screening

As shown in the two previous cases, the attachment and detachment of a relatively small soluble group (e.g., phosphate) of **1** can convert the solution of precursor to the hydrogel and versus versa, which leads us to test if the use of a relatively large soluble group can achieve similar phase transition. In order to evaluate the possible application of the visually observable change (i.e., gel-to-sol or sol-to-gel phase transition), we chose to conjugate **1** with a soluble β-lactam ring because a major class of antimicrobial agents relies on the strained β-lactam ring to react with penicillin binding proteins (PBPs) to inhibit cell wall synthesis and growth of bacteria. But β-Lactamases hydrolyze the four-member β-lactam ring and render the antibiotics ineffective and cause the most widespread antimicrobial drug resistance. For detecting β-lactamases and screening their inhibitors, we chose to use the event of hydrogelation to report the presence of β-lactamases.22 Figure 9 outlines the general principle and molecular design for a β-lactamase-catalyzed hydrogelation. Using the cephem nucleus as the linker, a hydrophilic group (e.g., glycine) connects a hydrogelator (**5b**) derived from **1** to afford the precursor (**5a**), which is too soluble to form a hydrogel. Upon the action of a β-lactamase, the β-lactam ring opens to release the hydrogelator (**5b**), which self-assembles in water into nanofibers to generate a hydrogel.

As shown in Figure S2 A and C, the precursor (**5a**), is too soluble to form a hydrogel (i.e., the precursor supplies too little hydrophobic interaction to self-assemble and gel water, Figure S2A and C). Upon the action of a β-lactamase, the β-lactam ring opens to release the hydrogelator (**5b**), which self-assembles in water and forms nanofibers to that result in a hydrogel (Figure S2B and D). The key feature of the design is to use a β-lactamase to generate a hydrogelator. By treating solution of **5a** with different types of bacteria cell lysates, we accurately identified the lysates containing β-lactamase based on this visual assay.22 This success not only promises an alternative approach to assay the β-lactamase (e.g., ESBL) in a more specific way via tailoring the structure of the precursors, but also confirms the versatility of **1** for offering a general motif to enable the self-assembly of other biofunctional molecules or groups.

NapFF-$NHCH_2CH_2OH$ for selective cell inhibition

Another hydrogelator (**6b**) derived from **1,** generated by an enzyme from its precursor (**6a**), can form the hydrogel inside cancer cells and inhibit cell growth.23 After verified that **6b** is an effective hydrogelator exhibiting a minimum gelation concentration (mgc) as low as 0.08 wt%, we designed and synthesized the precursor (**6a**) containing the hydrogelator and a cleavable butyric diacid, which forms an ester bond with the hydroxyl group on the aminoethanol end of **6b**. The butyric acid group acts as the enzymatic trigger for changing the overall balance of the hydrophobic and hydrophilic interactions and preventing the formation of the nanofibers of **6b** without enzymatic hydrolysis. The addition of the esterase to the solution of **6a** (0.08 wt%) at physiological temperature (37 °C) results in the formation of the hydrogel. Because the resulted hydrogelator (**6b**) lacks of the carboxylic acid group, the hydrogel is stable over wide range of pH (form 0 to 14). According to the rheological experiments and ^{1}H NMR analysis, the hydrogelation starts 6 minutes after the addition of the esterase when 68% of **6a** transforms to **6b**. The formed hydrogel of **6b** is transparent, which agrees with the TEM image of the hydrogel that shows the width of the nanofibers of about 25 nm.

Like compound **3a**, the molecule of **6a** is small enough to enter cells via passive diffusion (Figure 10). To evaluate the effect of **6a** against mammalian cell lines, we added **6a** into the culture of fibroblast cells (NIH3T3) or HeLa cells and measured the proliferation of the cells. As the MTT assay shown in Figure 11A, the number of the NIH3T3 cells barely decrease from the first day to the third day. On the contrary, the HeLa cells treated by **6a** displays decreased cell proliferation with the increase of the concentration of **6a** or time (Figure 11B), which is consistent with the observation of the change of cell morphology. A simple qualitative assay on the esterase expression in the HeLa cells and the fibroblast cells indicates that the level of the expression of esterase in HeLa cell is higher than that in the NIH3T3 cells.23 This result suggests that the relative high-level expression of the esterases in the HeLa cell promotes the quick built-up of **6b**, which self-assembles to form nanofibers. In addition, this result also indicates that self-assembly may amplify the relative small difference in the expression of enzymes. In a broad sense, the target of **6b** in this case is water in the cytosol; therefore it is possible to design a substrate to be susceptible to multiple enzymes to achieve more sophisticated controls (e.g. both spatial and temporal controls) for regulating cell fate.

NapFF conjugates with taxol for self-drug delivery

The exceptional capability of **1** to induce other molecules to self-assemble in water leads us to conjugate it with taxol, a sophisticate molecular anticancer agent.24 Considering the bulky size of taxol, we decide to connect taxol to NapFF via the “side-on” mode. To help create the site for the connection, a lysine residue links **1** to afford NapFFK. A tyrosine phosphate also extends from the C-terminal of NapFFK to afford **7**, which provides the enzymatic trigger and improves the solubility the final conjugate (**8a**). Scheme S3 shows the synthetic route and the structure of the conjugate (**8a**), which consists of the samogen (blue color), an enzyme-cleavable group (red), a linker (pink), and a taxol molecule (orange). As shown in Figure 12, upon the action of the enzyme, the precursor (**8a**) transforms into a hydrogelator (**8b**), which self-assembles to form nanofibers and affords a supramolecular hydrogel of the taxol. According to the TEM in Figure 12E, 5 min after the addition of the enzyme, the mixture already contains the nanofibers with a diameter of 20 nm, in addition to particle aggregates. The hydrogel of **8b** exhibits well-dispersed nanofiber networks with a uniform fiber width of 29 nm (Figure 12F).

As shown in Figure S3A, the activity of taxol, after conjugating with NapFFK, is conserved successfully in the precursor and the hydrogelator. Figure S3B shows the release profiles of

8b from its own gel. The slow-release and its cytotoxicity of **8b** suggests a way for self drug-delivery. Taking the advantage of the samogen (NapFFK in this case), this result represents the first example of enzyme instructed self-assembly and hydrogelation of complex, bioactive small molecules, which demonstrates a new, facile way to formulate highly hydrophobic drugs, such as taxol, into an aqueous form (e.g., hydrogel) without comprising their activity, and promises a general methodology to create therapeutic molecules that have a dual role as the delivery vehicle and the drug itself. This result also suggests that drug molecules are excellent candidates for conjugating with the samogens in the development of functional hydrogels or soft materials that promise various biomedical applications, including sustained or controlled drug release.

4. Several samogens share common features with NapFF

As discussed in previous sections, the key feature of **1** is the cooperative enhancement of non-covalent interactions due to multiple aromatic-aromatic interaction and hydrogen bonds. Therefore, if multiple aromatic-aromatic interactions and hydrogen bonds originate from their molecular structure, other small molecules should be able to self-assemble in water. In this section, we introduce a few examples (Scheme 3) bearing structural characteristics of **1**.

The enantiomer of NapFF

The structural isomer that would have (almost) identical behavior as **1** is its enantiomer Napff (**9**, f = D-phenylalanine).25 Thus, we synthesized **9** using D-phenylalanine and examined its properties. Compound **9** forms a clear hydrogel at the concentration of 1% and exhibit similar rheological behavior as **1** at the same concentration. The circular dichroism spectra of the hydrogels of **1** and **9** display a mirror image that agrees with their chirality.25 TEM images also reveal that **9** form nanofibers in water with the diameter of 20–46 nm (Figure 13), which is close to the nanofibers formed by **1**.

There is, however, a significant difference between the hydrogels of **1** and **9**. The hydrogel of **9** resists to protease-based digestive enzyme (e.g. proteinase K),25 a very useful property that allows the hydrogel of **9** to act as a potential medium for drug delivery. Using mice model and radioactive tracers, we found that the hydrogel formed by **9** exhibited good controlled release characteristics *in vivo*. For example, after subcutaneously injecting the hydrogel of **9** into the abdomens of rats, gel-encapsulated ^{125}I-NaI was released, and thereafter the blood concentration of ^{125}I-NaI was maintained within a narrow range during the first 12 hours after administration. SPECT images also showed that 4 hours after subcutaneous injection only about one-third of the ^{131}I-NaI solution remained in the injection site, whereas nearly two-thirds of the gel-encapsulated ^{131}I-NaI remained. Using the clinically used drug epidepride to replace NaI, we also found that the gel encapsulated ^{125}I-epidepride and ^{131}I-epidepride showed controlled release behavior *in vivo*. These results suggest that supramolecular hydrogels based on D-amino acids or D-peptides may lead to new types of biomaterials for sustained drug release.

A β-peptide as a structural isomer of NapFF

One of structural isomer of NapFF investigated by us belongs to β-peptides. Despite the considerable progress in the design and synthesis of β-peptides, the application of β-amino acids for controlling the bioavailability of supramolecular hydrogels remains little explored because the function of the β-amino acid derivative as a hydrogelator was unknown. We synthesized and characterized compound **10** that consists of two β-amino acids (β^3-homophenylglycine, β^3-Hphg)). **10** acts as a hydrogelator under proper conditions (e.g., concentration, temperature, and pH). For example, 5 mg of **10** in 1.0 mL of water forms a slightly opaque hydrogel (Figure 14A) by carefully adjusting pH or temperature (the pH

range and temperature of gel–sol phase transition are 6.2–6.5 and ~48 °C, respectively). This hydrogel is stable at room temperature for several months. As shown in Figure 14B, a wide range of sizes of the fibrils (ranging from 20 to 80 nm) constitute the matrices of the hydrogel. The small fibrils exhibit tendency to tangle with each other and form large bundles, which further confirms the stronger π-π stacking ability of β^3-HPhg, and agrees with its relative high storage modulus.26

Based on the knowledge that Nap-β^3-HPhg-β^3-HPhg (**10**) is a hydrogelator, we designed and synthesized a chimera of tripeptide derivative that consists of two β-amino acids (i.e., β^3-homophenylglycine) and one α-amino acid residue (i.e., tyrosine phosphate). The tripeptide derivative undergoes enzymatic hydrogelation *in vitro* and *in vivo*.27 Moreover, *in vivo* experiments revealed that the hydrogels formed by β-amino acid derivatives had a longer lifetime than that of hydrogels formed by α-amino acid derivatives. These results suggest that supramolecular hydrogels derived from the β-amino acid-derived samogen, Nap-β^3-HPhg-β^3-HPhg, could evolve into promising candidates for biomedical applications when long-term stability is required and the long-term biostability of β-peptide is established.

NapF-Glucosamine

One interesting case is that NapF can also act as a samogen to induce the self-assembly of a glycoside.28 As shown in Scheme 3, either Nap-L-phenylalaninae (NapF) or Nap-D-phenylalaninae (Napf) can connect to glucosamine via the formation of an amide bond to afford **11** or **12**. Both **11** and **12** are effective hydrogelators, which form the transparent hydrogels at 0.2 wt% (Figure S4A and B) and pH around 7. These two hydrogels are stable at room temperature for several months. Rheological measurement (Figure S4C and D) confirms that the value of storage modulus (G') of the hydrogel of **11** is larger than that of the hydrogel of **12**, the range of plateau of the hydrogel of **12** is wider than that of the hydrogel of **11**, suggesting that the hydrogel of **11** is slightly more viscoelastic, while the hydrogel of **12** is more tolerant to external force. The TEM images of the hydrogels, as shown in Figure S4E and F, reveal that the irregular small ribbons form large bundles and tangle with each other in the hydrogel of **11**, in addition to a small amount of helical fibers with diameters ranging from 27 to 55 nm. In the hydrogel of **12**, small rigid ribbons with diameters of 35–50 nm form well-distributed matrices. The different morphologies in both gels are likely resulted from their different structures. According to TEM images, compound **11** with an L-phenylalanine tends to aggregate and form larger bundles crosslinked network. We found that the resulted supramolecular hydrogelators exhibit good biocompatibility. More importantly, the resulting hydrogel of **11** assists wound healing and prevents the formation of scars on a mouse model. This result also supports the notion that the self-assembly of bioactive molecules, to form networks of nanofibers in the hydrogel could offer a useful and effective way to generate biomaterials.

5. Conclusion and perspective

In summary, we have demonstrated the versatility of several simple samogens, which serve as the building blocks of hydrogelators that promise many useful applications, including drug release, bacteria typing, wound healing, cell inhibition, and catalysis. An obvious opportunity is to use the known or potential samogens to conjugate with the vast pool of bioactive molecules and to enable molecular self-assembly in water for the development of molecular hydrogels. In fact, the recent development of molecular gelators has provided an array of possible samogens, which are based on either aromatic-aromatic interaction3,29or hydrophobic forces among alkyl chains.30 Because of their small sizes, the samogens discussed here can be modified easily. Therefore, it is feasible to make a large variety of molecular hydrogelators. Since the molecular arrangement in the nanofibers remains a

challenge, the accumulation of knowledge that is necessary for establishing, validating, and refining theoretical models of molecular self-assembly becomes necessary. The use of samogens for self-assembly not only provides rich opportunities to develop supramolecular materials, but also contributes to the interplay of the modeling and experimental design, which ultimately could lead to a more predictive theory or models for molecular self-assembly.[31] We expect that the collaboration of experimental scientists and theoreticians on the study of samogen-based hydrogelators will lead to rational design and development of molecular hydrogels for a variety of applications.

Supplementary Material

Refer to Web version on PubMed Central for supplementary material.

Acknowledgments

The works described were partially supported by Research Grant Council (Hong Kong), HFSP (RGP0056/2008), a star up fund from Brandeis University, NSF (MRSEC 0820492), and NIH (R01CA142746-01). Some of the images were taken at the Brandeis EM facility.

REFERENCES

1. Whitesides GM, Grzybowski B. Science. 2002; 295:2418–2421. [PubMed: 11923529]
2. Xia YN, Whitesides GM. Annu. Rev. Mater. Sci. 1998; 28:153–184.Yu TB, Bai JZ, Guan ZB. Angew. Chem.-Int. Edit. 2009; 48:1097–1101.Yin P, Hariadi RF, Sahu S, Choi HMT, Park SH, LaBean TH, Reif JH. Science. 2008; 321:824–826. [PubMed: 18687961] Jung, JH.; Shinkai, S. Templates in Chemistry I. Vol. Vol. 248. Berlin: Springer-Verlag Berlin; 2004. p. 223-260.Zang L, Che YK, Moore JS. Accounts Chem. Res. 2008; 41:1596–1608.Caruso F, Yang WJ, Trau D, Renneberg R. Langmuir. 2000; 16:8932–8936.Elbert DL, Herbert CB, Hubbell JA. Langmuir. 1999; 15:5355–5362.Zhang SG. Nat. Biotechnol. 2003; 21:1171–1178. [PubMed: 14520402] Hartgerink JD, Beniash E, Stupp SI. Proc. Natl. Acad. Sci. U. S. A. 2002; 99:5133–5138. [PubMed: 11929981] Takaoka Y, Sakamoto T, Tsukiji S, Narazaki M, Matsuda T, Tochio H, Shirakawa M, Hamachi I. Nat. Chem. 2009; 1:557–561. [PubMed: 21378937] Geiger C, Stanescu M, Chen LH, Whitten DG. Langmuir. 1999; 15:2241–2245.Chen J, McNeil AJ. J. Am. Chem. Soc. 2008; 130 16496−+ Zheng G, Chen J, Li H, Glickson JD. Proc. Natl. Acad. Sci. U. S. A. 2005; 102:17757–17762. [PubMed: 16306263]
3. Xue PC, Lu R, Zhao L, Xu DF, Zhang XF, Li KC, Song ZG, Yang XC, Takafuji M, Ihara H. Langmuir. 2010; 26:6669–6675. [PubMed: 19957943]
4. Dastidar P. Chem. Soc. Rev. 2008; 37:2699–2715. [PubMed: 19020683] Estroff LA, Hamilton AD. Chem. Rev. 2004; 104:1201–1217. [PubMed: 15008620] Nagarkar RP, Hule RA, Pochan DJ, Schneider JP. Biopolymers. 2010; 94:141–155. [PubMed: 20091872] Rajagopal K, Schneider JP. Curr. Opin. Struct. Biol. 2004; 14:480–486. [PubMed: 15313243] Terech P, Weiss RG. Chem. Rev. 1997; 97:3133–3159. [PubMed: 11851487]
5. Yang Z, Liang G, Xu B. Accounts Chem. Res. 2008; 41:315–326.
6. Hoffman AS. Adv. Drug Deliv. Rev. 2002; 54:3–12. [PubMed: 11755703] Lutolf MP, Hubbell JA. Nat. Biotechnol. 2005; 23:47–55. [PubMed: 15637621] Peppas NA, Langer R. Science. 1994; 263:1715–1720. [PubMed: 8134835]
7. Cui HG, Webber MJ, Stupp SI. Biopolymers. 2010; 94:1–18. [PubMed: 20091874] Williams RJ, Mart RJ, Ulijn RV. Biopolymers. 2010; 94:107–117. [PubMed: 20091879] Nagarkar RP, Hule RA, Pochan DJ, Schneider JP. Biopolymers. 94:141–155. [PubMed: 20091872] Yang YL, Khoe U, Wang XM, Horii A, Yokoi H, Zhang SG. Nano Today. 2009; 4:193–210.
8. Schneider J. Biopolymers. 2010; 94:III–III. [PubMed: 20091880]
9. Lin Y, Kachar B, Weiss RG. J. Am. Chem. Soc. 1989; 111:5542–5551.Aoki M, Murata K, Shinkai S. Chem. Lett. 1991:1715–1718.Menger FM, Venkatasubban KS. J. Org. Chem. 1978; 43:3413–3414.

10. Zhang Y, Gu HW, Yang ZM, Xu B. J. Am. Chem. Soc. 2003; 125:13680–13681. [PubMed: 14599204]
11. Burley SK, Petsko GA. Science. 1985; 229:23–28. [PubMed: 3892686]
12. Ma ML, Kuang Y, Gao Y, Zhang Y, Gao P, Xu B. J. Am. Chem. Soc. 2010; 132:2719–2728. [PubMed: 20131781]
13. Inouye, H.; Kirschner, DA.; Masters; Buxbaum, JD.; Pepys; Kisilevsky; Kelly; Maury; Westermark; Ciba Fdn, CFCF. Nature and Origin of Amyloid Fibrils. Vol. Vol. 199. Chichester: John Wiley & Sons Ltd; 1996. p. 22-39.
14. Balbach JJ, Ishii Y, Antzutkin ON, Leapman RD, Rizzo NW, Dyda F, Reed J, Tycko R. Biochemistry. 2000; 39:13748–13759. [PubMed: 11076514]
15. Reches M, Gazit E. Science. 2003; 300:625–627. [PubMed: 12714741]
16. Yuasa T, Nogawa M, Kimura S, Yokota A, Sato K, Segawa H, Kuroda J, Maekawa T. Clin. Cancer Res. 2005; 11:853–859. [PubMed: 15701876]
17. Yang ZM, Xu KM, Wang L, Gu HW, Wei H, Zhang MJ, Xu B. Chem. Commun. 2005:4414–4416.
18. Yang Z, Liang G, Guo Z, Xu B. Angew. Chem.-Int. Edit. 2007; 46:8216–8219.
19. Wang QG, Yang ZM, Gao Y, Ge WW, Wang L, Xu B. Soft Matter. 2008; 4:550–553.
20. Yang ZM, Liang GL, Wang L, Xu B. J. Am. Chem. Soc. 2006; 128:3038–3043. [PubMed: 16506785]
21. Yang ZM, Ho PL, Liang GL, Chow KH, Wang QG, Cao Y, Guo ZH, Xu B. J. Am. Chem. Soc. 2007; 129:266–267. [PubMed: 17212393]
22. Yang ZM, Xu KM, Guo ZF, Guo ZH, Xu B. Adv. Mater. 2007; 19 3152−+
23. Gao Y, Kuang Y, Guo ZF, Guo ZH, Krauss IJ, Xu B. J. Am. Chem. Soc. 2009; 131 13576−+
24. Liang GL, Yang ZM, Zhang RJ, Li LH, Fan YJ, Kuang Y, Gao Y, Wang T, Lu WW, Xu B. Langmuir. 2009; 25:8419–8422. [PubMed: 20050040]
25. Yang ZM, Liang GL, Xu B. Chem. Commun. 2006:738–740.
26. Yang ZM, Liang GL, Ma ML, Gao Y, Xu B. Small. 2007; 3:558–562. [PubMed: 17323399]
27. Yang ZM, Liang GL, Ma ML, Abbah AS, Lu WW, Xu B. Chem. Commun. 2007:843–845.
28. Cheng G, Castelletto V, Moulton CM, Newby GE, Hamley IW. Langmuir. 2010; 26:4990–4998. [PubMed: 20073495] Chen L, Morris K, Laybourn A, Elias D, Hicks MR, Rodger A, Serpell L, Adams DJ. Langmuir. 2010; 26:5232–5242. [PubMed: 19921840] Wang GT, Lin JB, Jiang XK, Li ZT. Langmuir. 2009; 25:8414–8418. [PubMed: 19284767] Tang C, Smith AM, Collins RF, Ulijn RV, Saiani A. Langmuir. 2009; 25:9447–9453. [PubMed: 19537819] Chen Q, Lv YX, Zhang DQ, Zhang GX, Liu CY, Zhu DB. Langmuir. 2010; 26:3165–3168. [PubMed: 19842630] Shome A, Debnath S, Das PK. Langmuir. 2008; 24:4280–4288. [PubMed: 18324868]
29. Roy S, Dasgupta A, Das PK. Langmuir. 2007; 23:11769–11776. [PubMed: 17918973] Meister A, Bastrop M, Koschoreck S, Garamus VM, Sinemus T, Hempel G, Drescher S, Dobner B, Richtering W, Huber K, Blume A. Langmuir. 2007; 23:7715–7723. [PubMed: 17547425] Escuder B, Marti S, Miravet JF. Langmuir. 2005; 21:6776–6787. [PubMed: 16008387] George M, Funkhouser GP, Weiss RG. Langmuir. 2008; 24:3537–3544. [PubMed: 18278965] Wang YB, Zhan CL, Fu HB, Li X, Sheng XH, Zhao YS, Xiao DB, Ma Y, Ma JS, Yao JN. Langmuir. 2008; 24:7635–7638. [PubMed: 18582139] Suzuki M, Saito H, Hanabusa K. Langmuir. 2009; 25:8579–8585. [PubMed: 19284771]
30. Johnson ER, Keinan S, Mori-Sa'nchez P, Contreras-Garcı'a J, Cohen AJ, Yang W. J. Am. Chem. Soc. 2010; 132:6498–6506. [PubMed: 20394428]

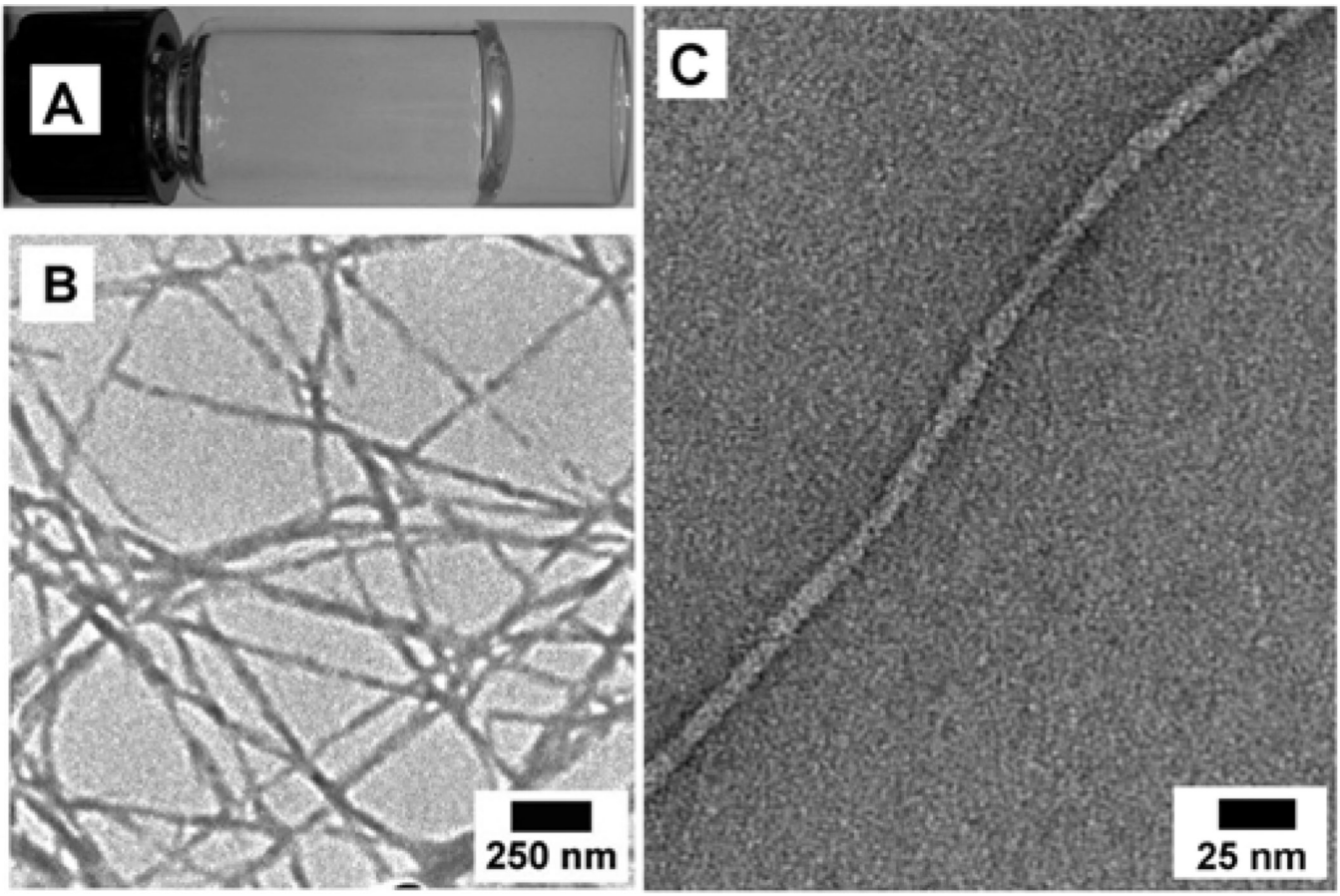

Figure 1.
(A) Optical image, (B) TEM image, (C) negative-stained TEM image of the hydrogel of **1** (0.6 wt%).

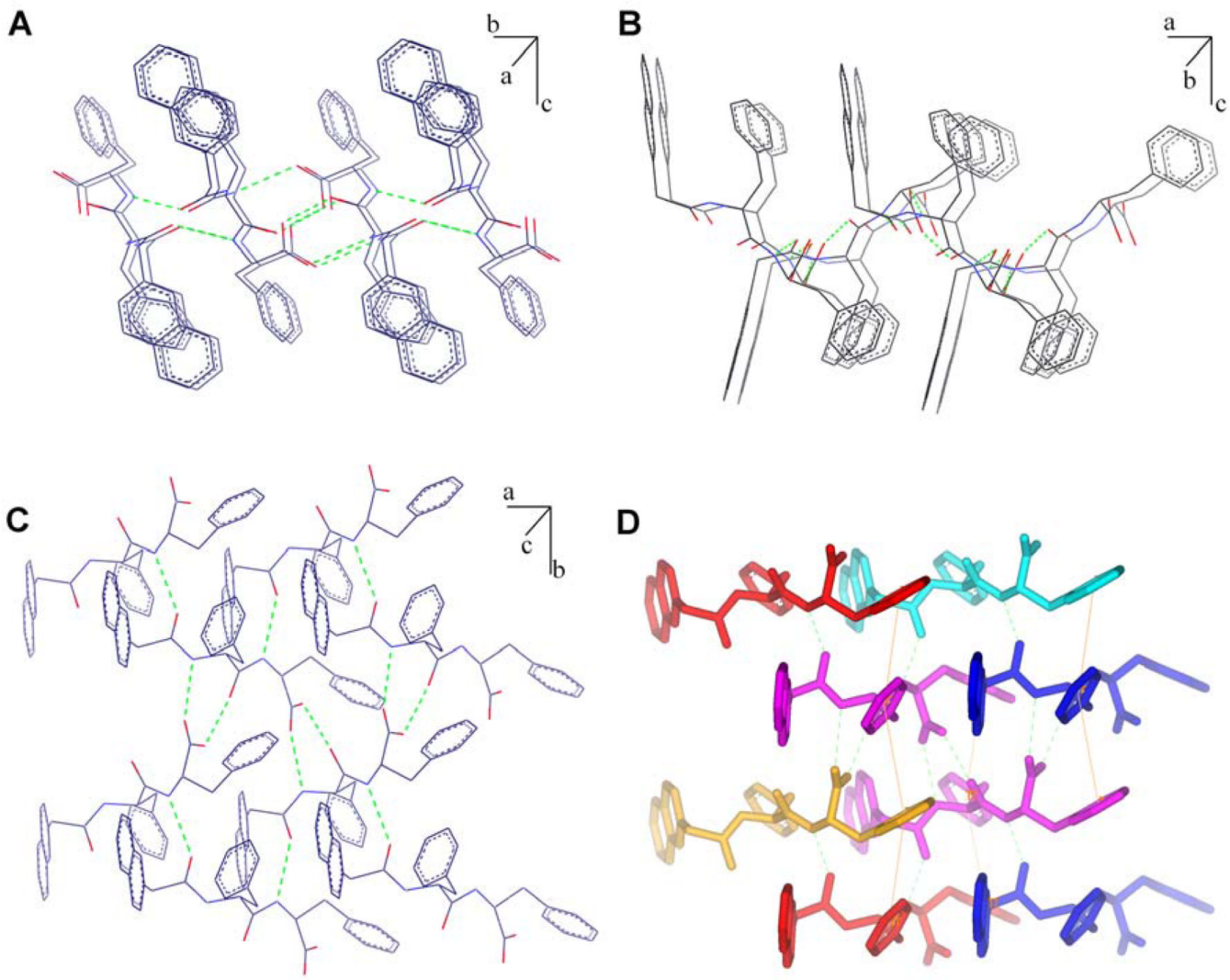

Figure 2.
The molecular packing and hydrogen bonds in the crystal of **1** (recrystallized from ethanol). View from (A) a-axis; (B) b-axis; (C) c-axis; and (D) view from c-axis to show the hydrogen bonding (green dot lines) of one molecule with other four molecules and some aromatic-aromatic interactions (yellow lines).

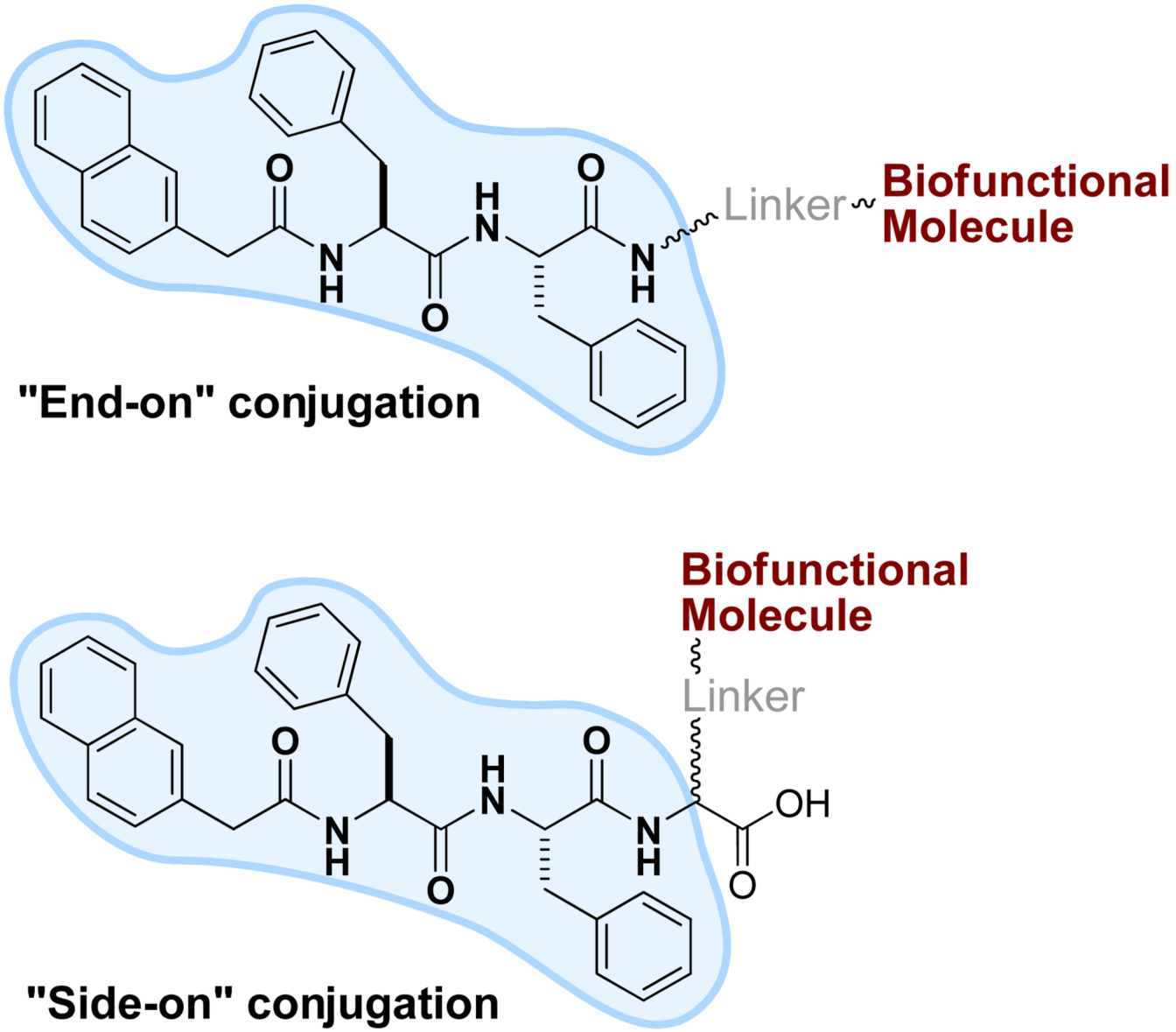

Figure 3.
Illustration of the modes for linking bioactive molecules to NapFF (**1**), the samogen.

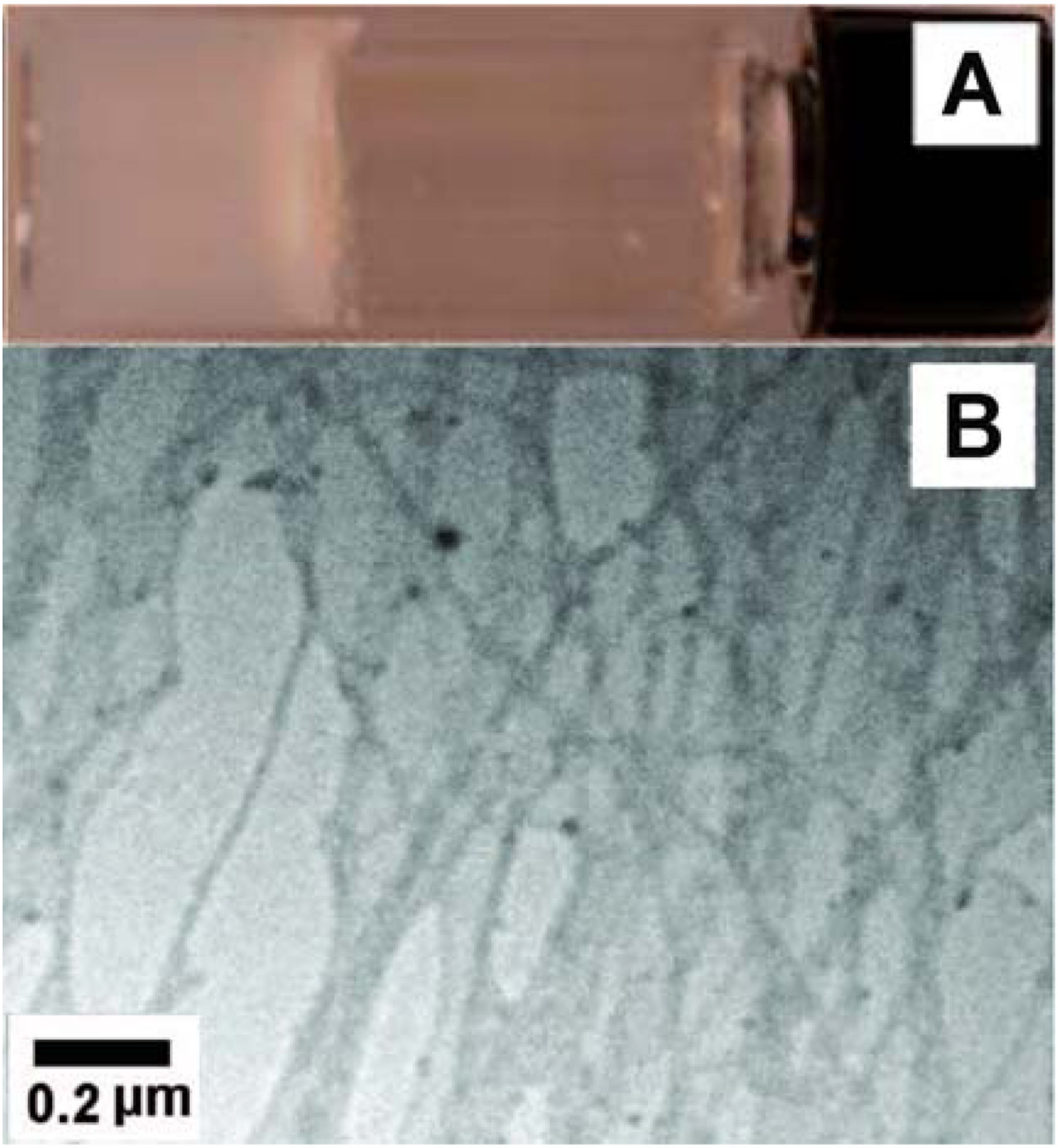

Figure 4.
The optical (A) and TEM (B) images of the hydrogel formed by **2** (1.0 wt% and pH 6.5).

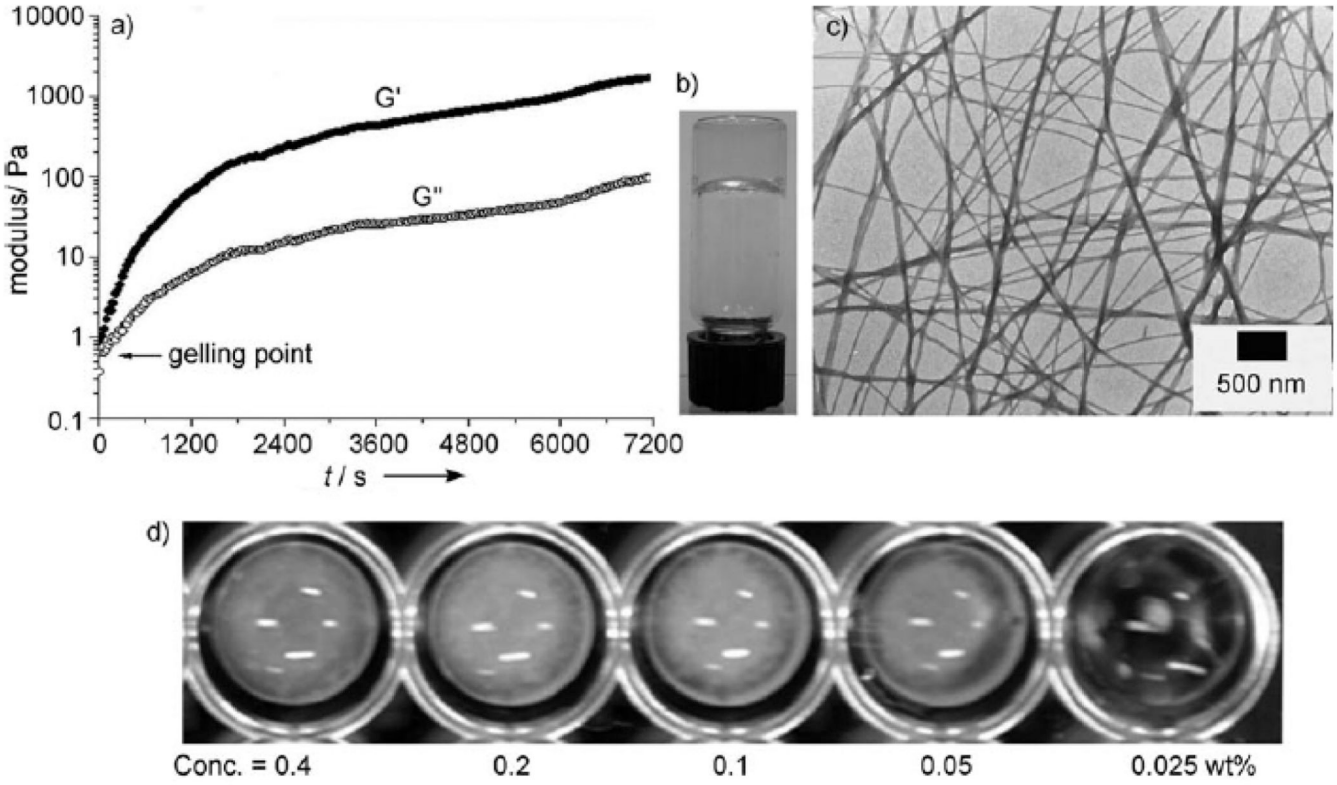

Figure 5.

A) Oscillatory rheology of a PBS buffer solution containing 6.91 mM (0.5 wt%,) of **3a** and 10 μL of enzyme solution (14U/μL), pH 7.4, 25.8 °C; B) optical and C) TEM images of the hydrogel formed by **3b** through enzymatic gelation in PBS buffer solution (0.5 wt%); D) enzymatic conversion of **3a** into **3b** with the addition of alkaline phosphatase (700 U/mL) to PBS buffer solutions containing different concentrations of **3a**.

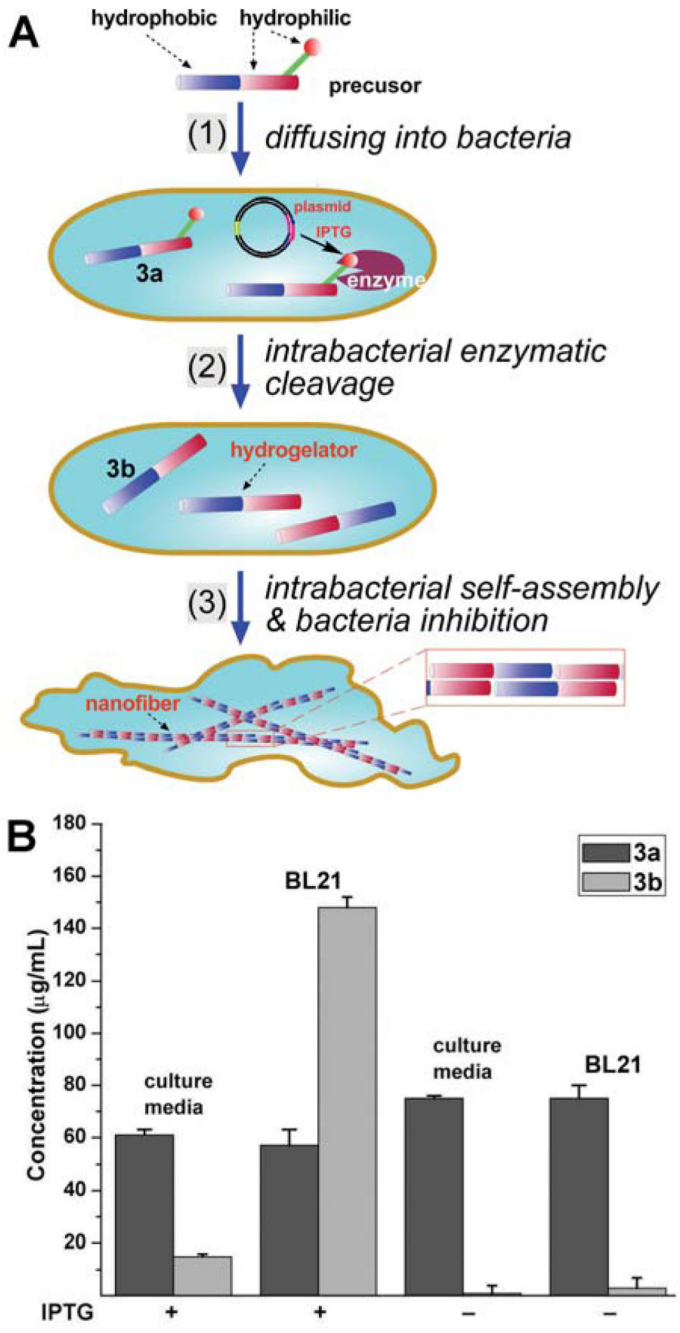

Figure 6.

A) Schematic representation of intrabacteria nanofiber formation leading to hydrogelation and the inhibition of bacterial growth. B) Concentrations of **3a** and **3b** in the culture medium and within the *E. Coli* (BL21, plasmid+, IPTG+ or IPTG−). Adapted with permission from ref.17. Copyright Wiley-VCH 2007.

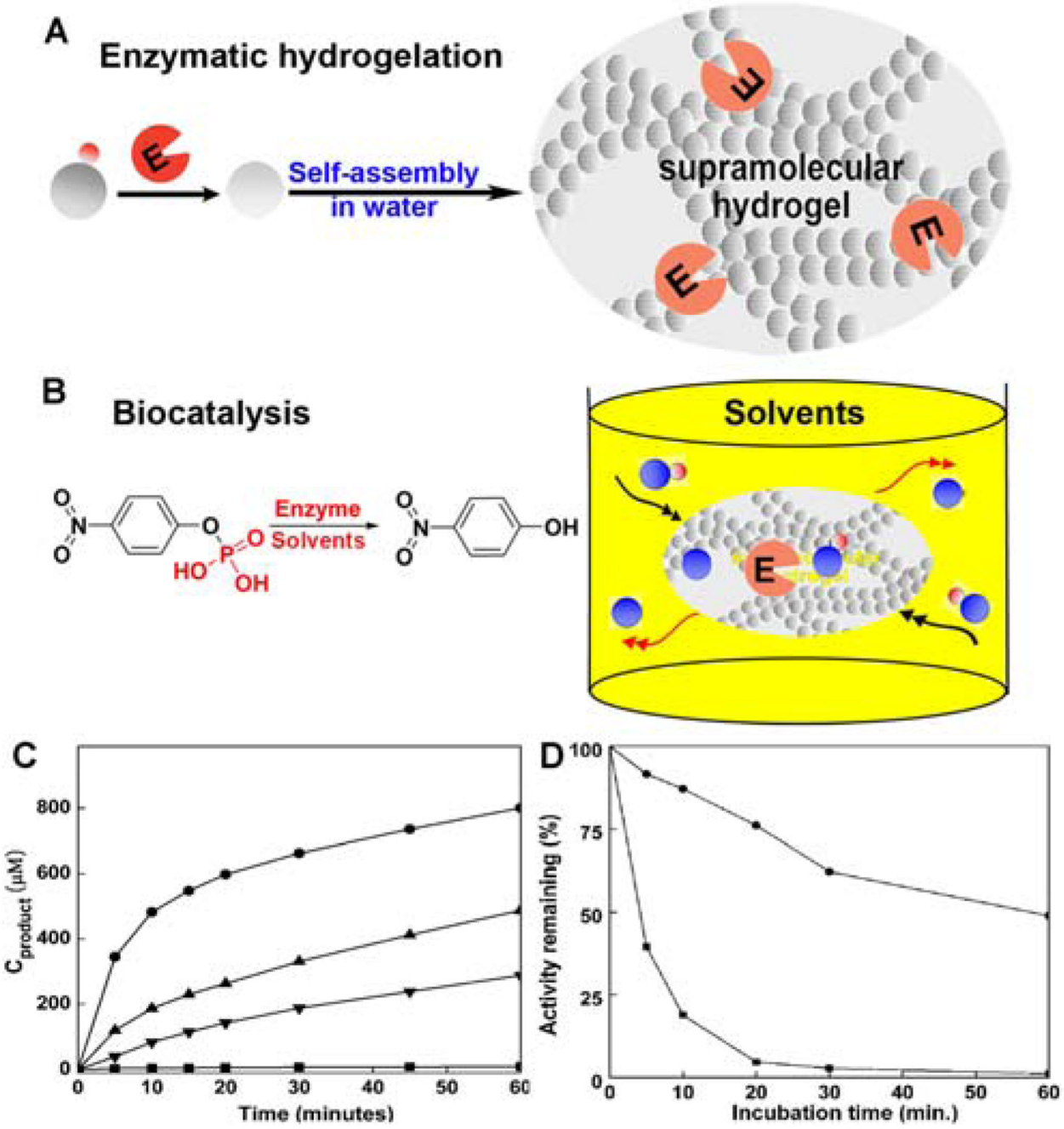

Figure 7.

(A) Illustration to show the location of the enzyme after the formation of the nanofibers in the hydrogel. (B) The acid phosphatase in hydrogel to catalyze the conversion of the substrate (O-phospho-nitrophenol, represented by the blue sphere plus red dot) to the product (nitrophenol, represented by the blue sphere) in organic media. (C) The hydrolysis of the substrate (10 mM) catalyzed by AP (within the gel, 20 μg/L) in chloroform (solid circles), toluene (up triangles), and n-octane (down triangles), and AP (free) in water (squares). (D) The remained activity of AP (within the gel, solid circles) and AP (free) (squares) in water after incubation at 60 °C at various time. Adapted with permission from ref.18. Copyright RSC 2008.

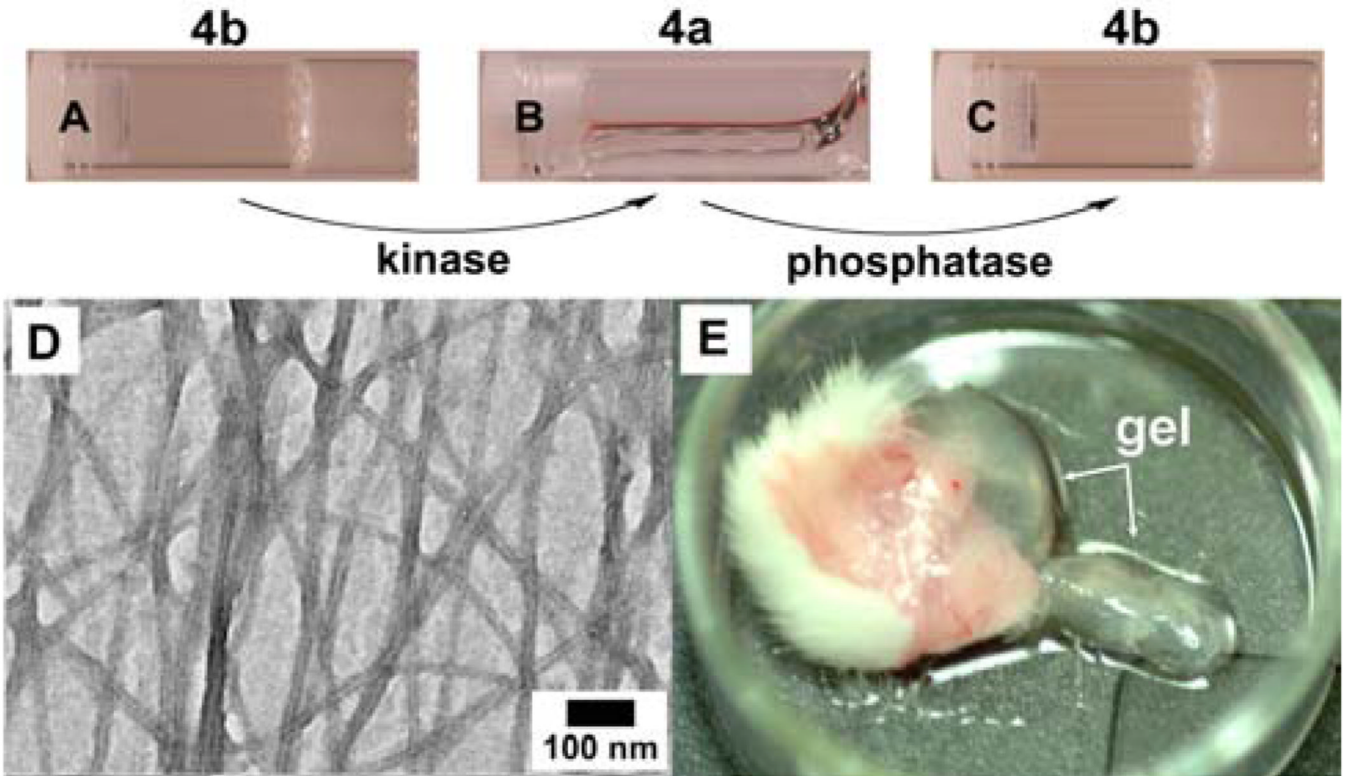

Figure 8.

Optical images (A) hydrogel of **4b**; (B) the solution obtained after adding a kinase to the gel of **4b**; and (C) hydrogel of **4b** formed by using phosphatase to treat 4a. (D)TEM images of the hydrogel of **4b** formed by using phosphatase to treat **4a**. (E) Optical image of the hydrogel formed subcutaneously 1 hour after injecting **4a** into the mice. Adapted with permission from ref.19. Copyright ACS 2006.

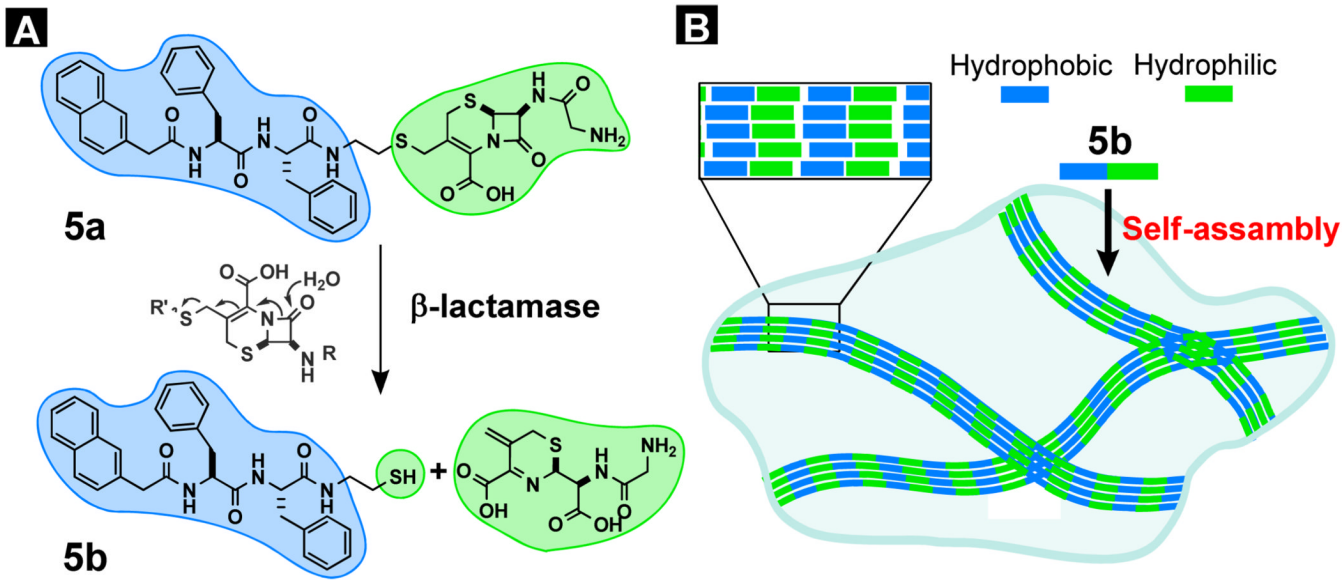

Figure 9.
(A) Illustration of the design of a substrate of β-lactamase (Bla) as the precursor of a hydrogelator; the opening of β-lactam ring catalyzed by Bla; (B) one possible mode of the self-assembly of the hydrogelator and the formation of the hydrogel.

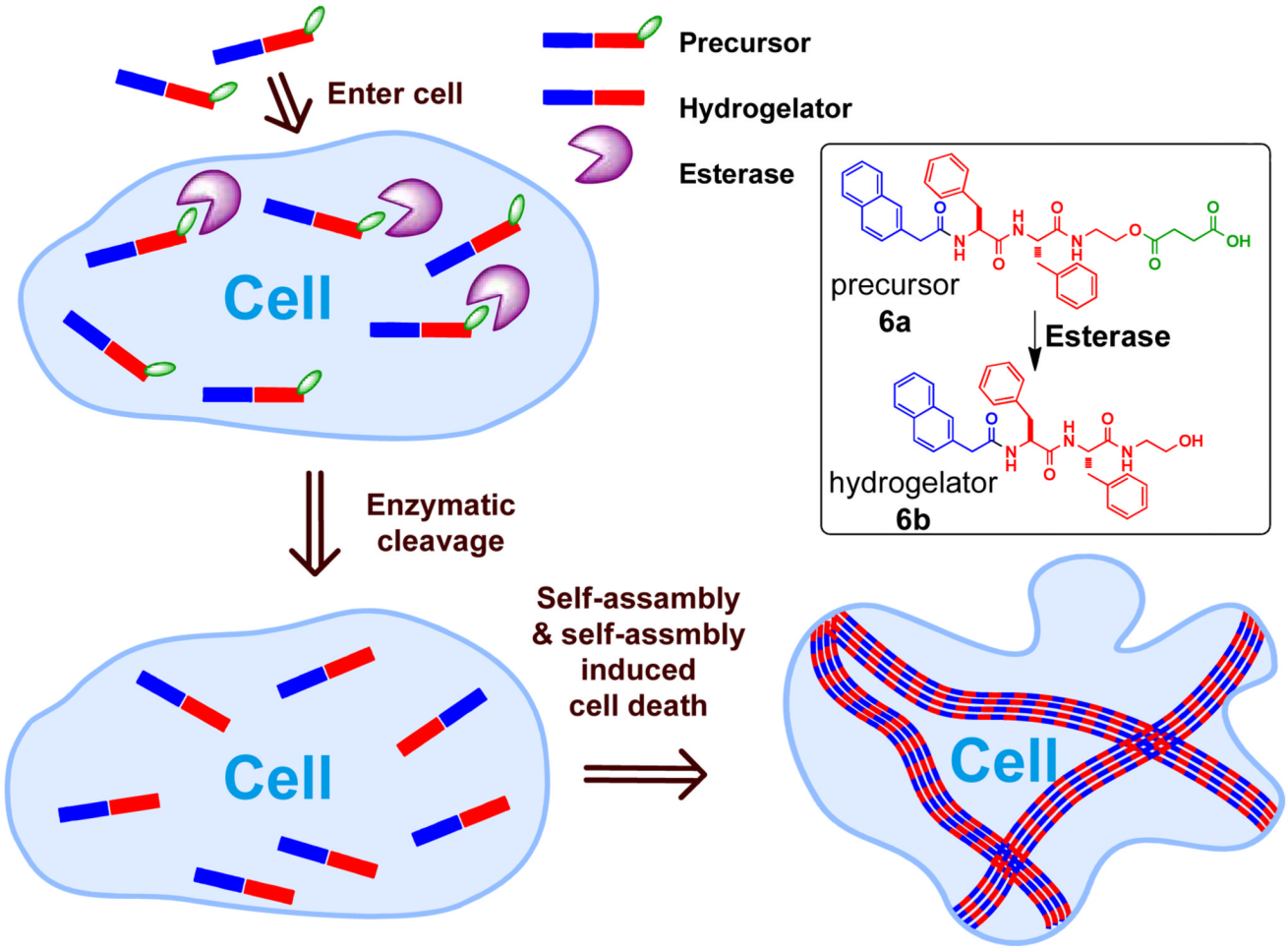

Figure 10.
The illustration of enzyme catalyzed intracellular hydrogelation as well as the chemical structures and the graphic representations of the precursor (**6a**) and the hydrogelator (**6b**).

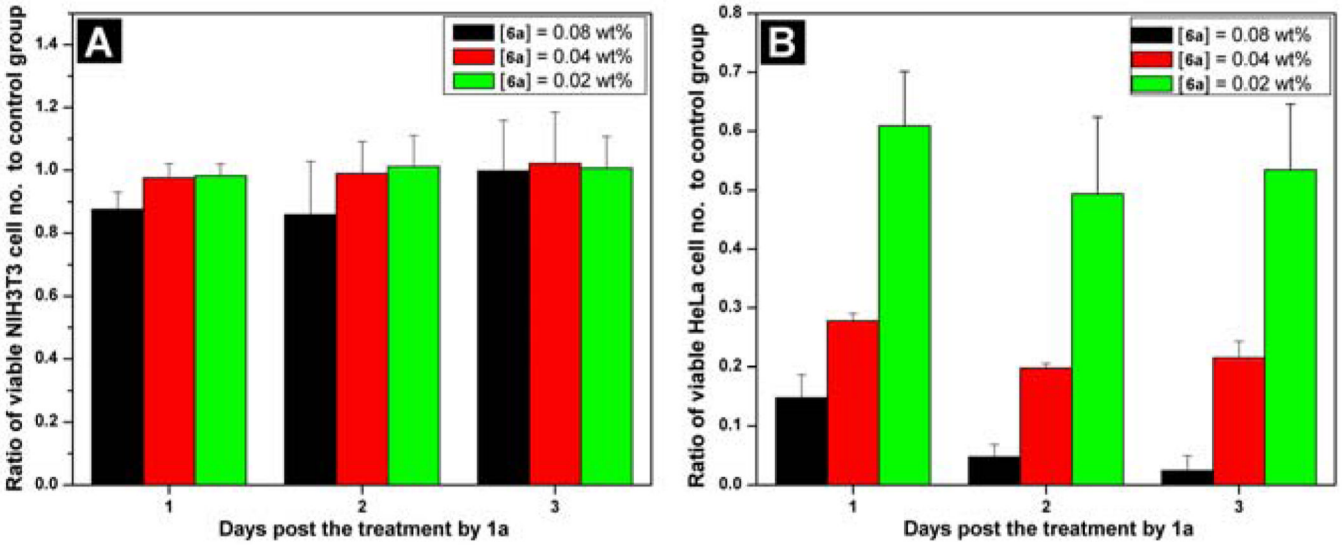

Figure 11.
MTT assays of (A) NIH3T3 cells and (B) HeLa cells treated with **6a** at concentrations of 0.08 wt%, 0.04 wt%, and 0.02 wt%. Adapted with permission from ref.21. Copyright Wiley-VCH 2007.

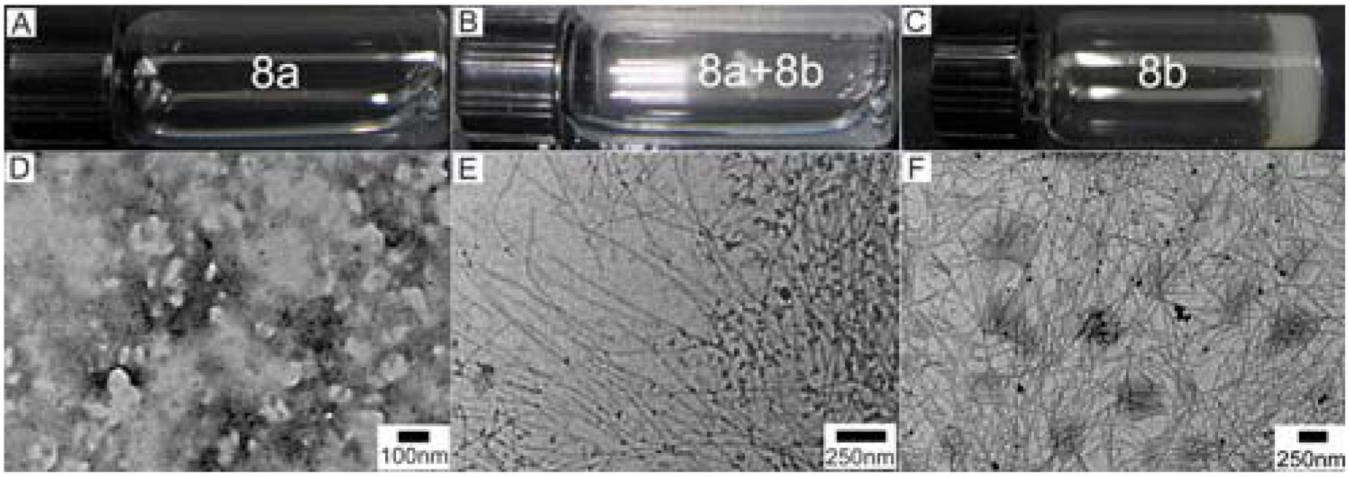

Figure 12.
Optical (A–C) and the corresponding transmission electron microscopic (TEM) images (D–F) of the solution of **8a** with [**8a**] = 1.0 wt % (A, D); the solution of **8a** at 5 min after the addition of alkaline phosphatase (ALP) (B, E); and the hydrogel of **8b** overnight after the addition of ALP (C, F). Adapted with permission from ref.22. Copyright ACS 2009.

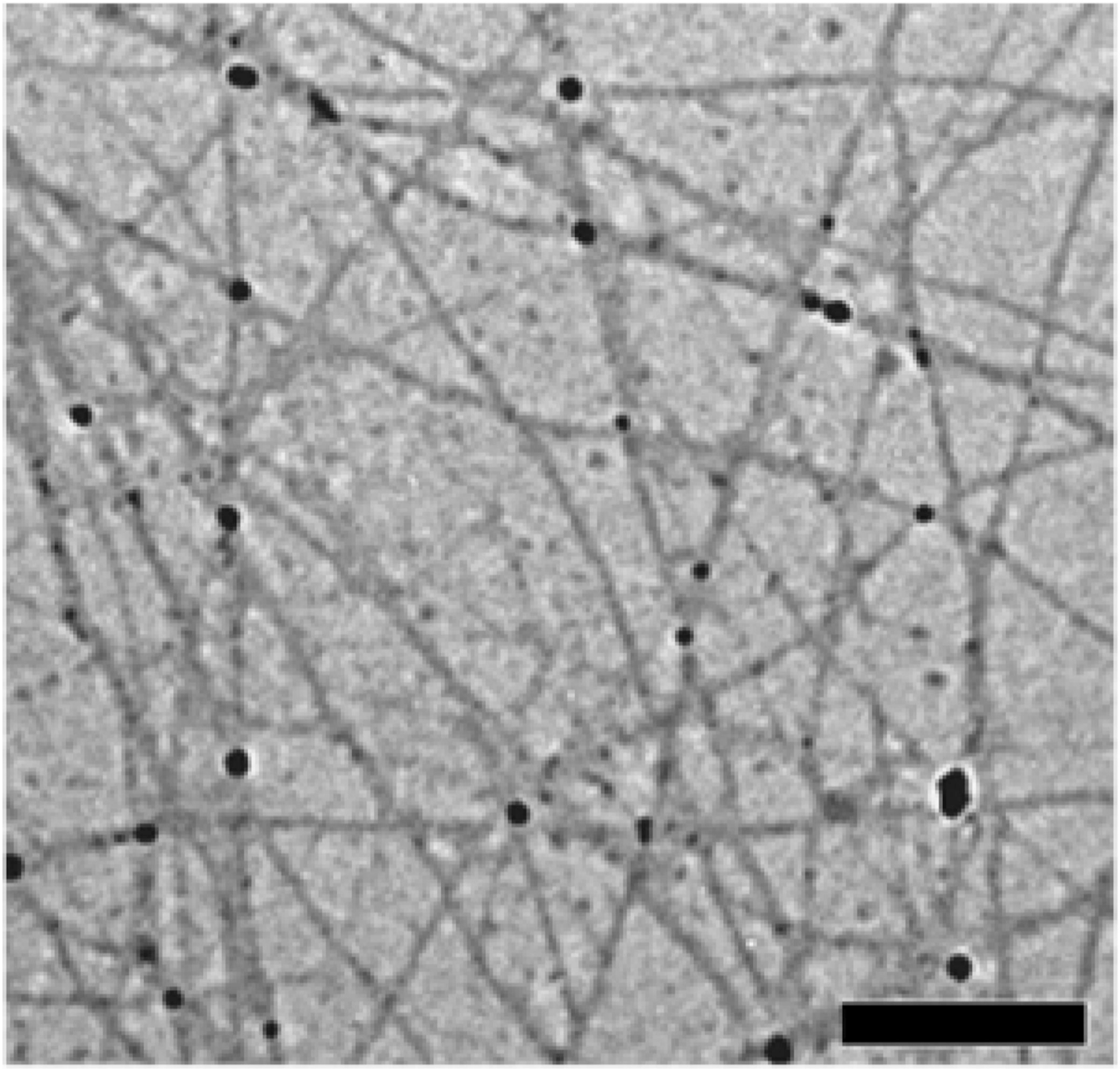

Figure 13.
TEM images of the nanofiber matrices in the hydrogel of Napff (**9**) (scale bar = 500 nm).

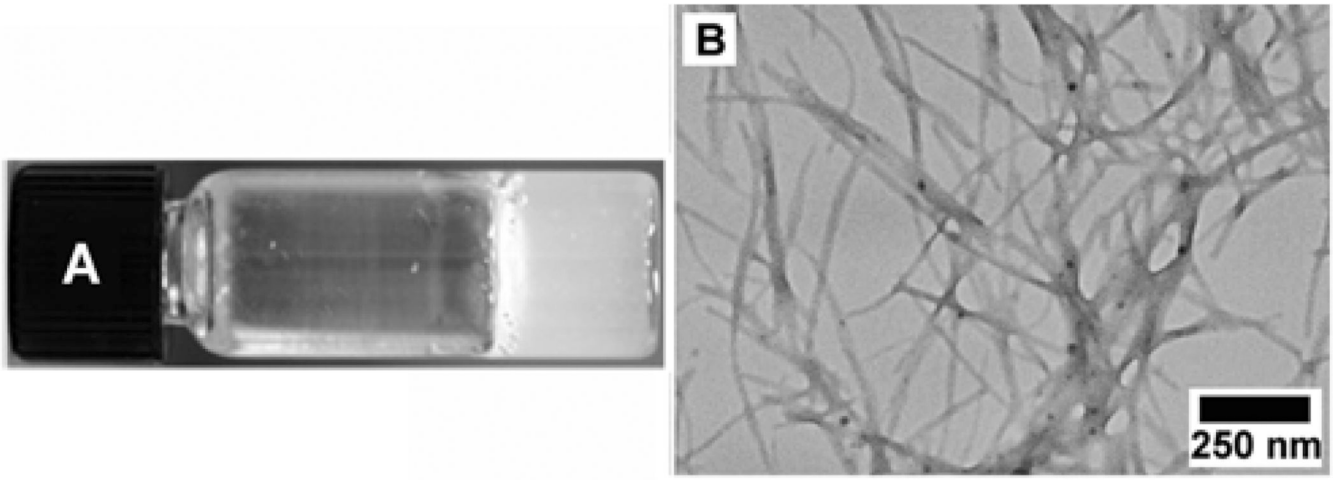

Figure 14.
(A) Optical image of the hydrogel formed by **10**. (B) TEM image of the hydrogel of **10**.

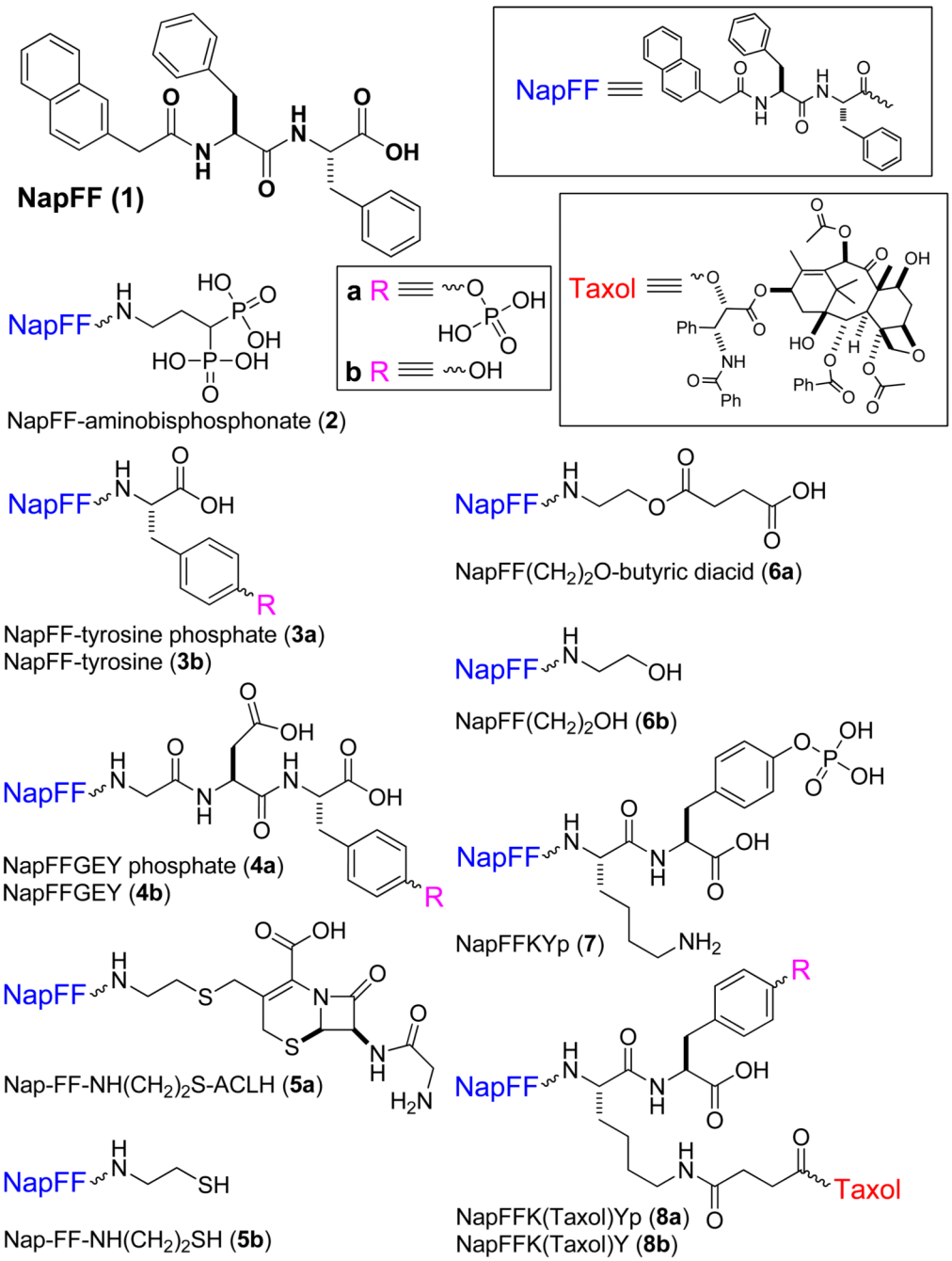

Scheme 1.
Molecular hydrogelators derived from NapFF (**1**).

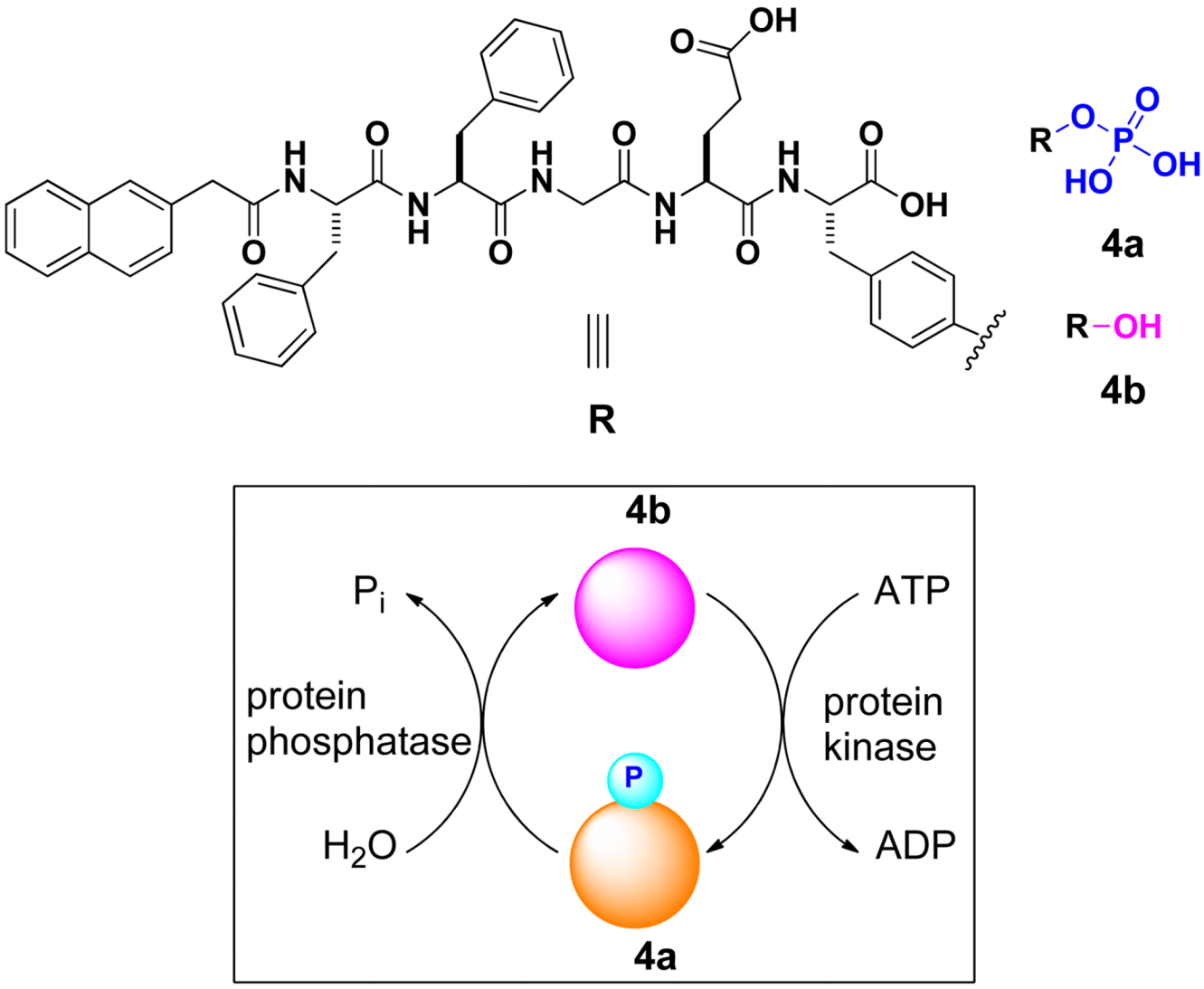

Scheme 2.
The structure of the substrates of kinase and phosphatase.

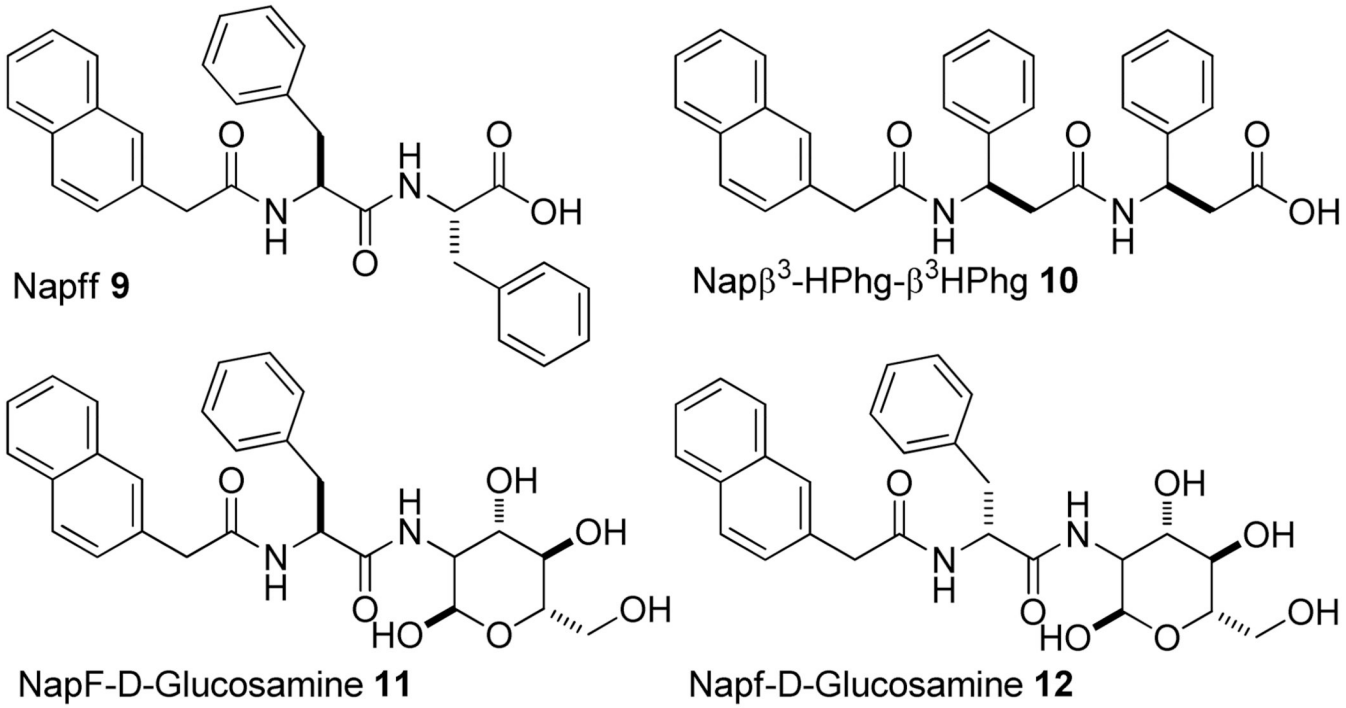

Scheme 3.
Hydrogelators similar to NapFF.